

See discussions, stats, and author profiles for this publication at: <https://www.researchgate.net/publication/224947229>

# Characterization of the Function of Cytoglobin as an Oxygen-Dependent Regulator of Nitric Oxide Concentration

ARTICLE *in* BIOCHEMISTRY · MAY 2012

Impact Factor: 3.02 · DOI: 10.1021/bi300291h · Source: PubMed

---

CITATIONS

22

---

READS

52

8 AUTHORS, INCLUDING:



[Xiaoping Liu](#)

The Ohio State University

62 PUBLICATIONS 3,327 CITATIONS

SEE PROFILE



[Craig Hemann](#)

The Ohio State University

57 PUBLICATIONS 1,764 CITATIONS

SEE PROFILE



[Lawrence Druhan](#)

The Ohio State University

46 PUBLICATIONS 1,489 CITATIONS

SEE PROFILE

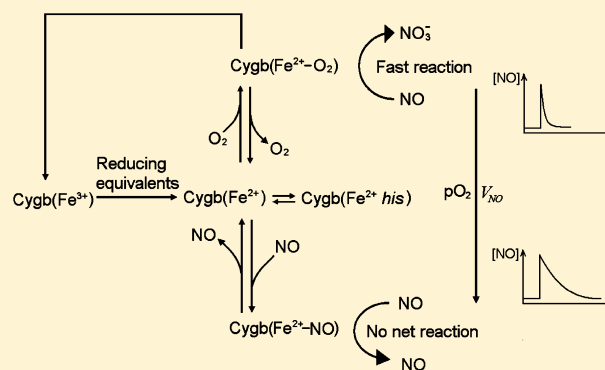
# Characterization of the Function of Cytoglobin as an Oxygen-Dependent Regulator of Nitric Oxide Concentration

Xiaoping Liu,<sup>\*,†,‡</sup> Douglas Follmer,<sup>†</sup> Joseph R. Zweier,<sup>†</sup> Xin Huang,<sup>†</sup> Craig Hemann,<sup>†</sup> Kerui Liu,<sup>†</sup> Lawrence J. Druhan,<sup>§</sup> and Jay L. Zweier<sup>\*,†,‡</sup>

<sup>†</sup>Davis Heart and Lung Research Institute and <sup>‡</sup>Department of Internal Medicine, The Ohio State University College of Medicine, 473 West 12th Avenue, Columbus, Ohio 43210, United States

<sup>§</sup>Department of Anesthesiology, The Ohio State University College of Medicine, 410 West 10th Avenue, Columbus, Ohio 43210, United States

**ABSTRACT:** The endogenous vasodilator nitric oxide (NO) is metabolized in tissues in an O<sub>2</sub>-dependent manner. This regulates NO levels in the vascular wall; however, the underlying molecular basis of this O<sub>2</sub>-dependent NO consumption remains unclear. While cytoglobin (Cygb) was discovered a decade ago, its physiological function remains uncertain. Cygb is expressed in the vascular wall and can consume NO in an O<sub>2</sub>-dependent manner. Therefore, we characterize the process of the O<sub>2</sub>-dependent consumption of NO by Cygb in the presence of the cellular reductants and reducing systems ascorbate (Asc) and cytochrome P<sub>450</sub> reductase (CPR), measure rate constants of Cygb reduction by Asc and CPR, and propose a reaction mechanism and derive a related kinetic model for this O<sub>2</sub>-dependent NO consumption involving Cygb(Fe<sup>3+</sup>) as the main intermediate reduced back to ferrous Cygb by cellular reductants. This kinetic model expresses the relationship between the rate of O<sub>2</sub>-dependent consumption of NO by Cygb and rate constants of the molecular reactions involved. The predicted rate of O<sub>2</sub>-dependent consumption of NO by Cygb is consistent with experimental results supporting the validity of the kinetic model. Simulations based on this kinetic model suggest that the high efficiency of Cygb in regulating the NO consumption rate is due to the rapid reduction of Cygb by cellular reductants, which greatly increases the rate of consumption of NO at higher O<sub>2</sub> concentrations, and binding of NO to Cygb, which reduces the rate of consumption of NO at lower O<sub>2</sub> concentrations. Thus, the coexistence of Cygb with efficient reductants in tissues allows Cygb to function as an O<sub>2</sub>-dependent regulator of NO decay.



Cytoglobin (Cygb) was discovered nearly 10 years ago as a fourth globin type expressed in mammals.<sup>1–3</sup> As seen for three other globins [hemoglobin (Hb), myoglobin (Mb), and neuroglobin (Ngb)], small gas molecules such as oxygen (O<sub>2</sub>), carbon monoxide (CO), and nitric oxide (NO) reversibly bind to the heme iron of Cygb. However, unlike the pentacoordinated hemoglobin and myoglobin, the histidine at position 7 of helix E, His (E7), in Cygb forms the internal sixth (distal) ligand to the heme iron in both the ferric (Fe<sup>3+</sup>) and the ferrous (Fe<sup>2+</sup>) forms in the absence of an external ligand.<sup>4</sup> Cygb is upregulated in tissues upon hypoxia.<sup>5,6</sup> It has been suggested that Cygb may play a role in storing O<sub>2</sub>, facilitating O<sub>2</sub> diffusion, detoxifying reactive oxygen species, acting as an O<sub>2</sub> sensor, and functioning as an NO dioxygenase.<sup>1,2,4,7–12</sup>

Cygb is predominantly expressed in fibroblasts and related cell types in different organs and tissues.<sup>1,3,13</sup> In blood vessels, recent evidence has shown that Cygb is expressed not only in adventitial fibroblasts but also in smooth muscle cells, playing a role in vascular NO catabolism,<sup>9</sup> and it may also function as a nitrite reductase in the vascular wall.<sup>14,15</sup> It was recently demonstrated that the extent of vascular NO catabolism is

reduced when the O<sub>2</sub> concentration is decreased.<sup>16</sup> The rate of O<sub>2</sub>-dependent NO consumption was found to be high enough to regulate the NO concentration and the diffusion distance in the vascular wall.<sup>16,17</sup> Because NO is a potent endogenous vasodilator that dilates blood vessels in a dose-dependent manner, an increased NO diffusion distance or an increase in the level of NO in hypoxia will induce blood vessel dilation, allowing more blood to flow through the vessel resulting in more O<sub>2</sub> being delivered to the hypoxic tissue.<sup>18–20</sup>

The Cygb concentration in tissue is in the micromolar range.<sup>8,10,21–23</sup> It has been shown that ferric Cygb (metCygb) can be reduced by cellular reductants such as ascorbate (Asc), cytochrome P<sub>450</sub> reductase (CPR), cytochrome b<sub>5</sub> (Cyto b<sub>5</sub>), and novel cytochrome b<sub>5</sub> oxidoreductase at a rate significantly higher than the rate of reduction of ferric myoglobin (metMb) and ferric neuroglobin (metNgb).<sup>10</sup> In the presence of O<sub>2</sub>, reduced Cygb binds O<sub>2</sub> to form oxyCygb that rapidly reacts

Received: February 29, 2012

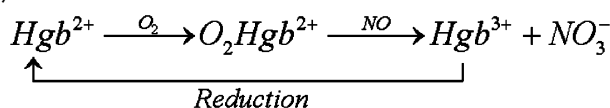
Revised: April 19, 2012

Published: May 11, 2012



with NO generating metCygb and nitrate in an O<sub>2</sub>-dependent manner. This process can allow Cygb to efficiently metabolize NO at low micromolar Cygb concentrations. The rate of consumption of NO by Cygb would be limited by the need to reduce metCygb to its ferrous form,<sup>8</sup> but the rate of Cygb-mediated NO consumption may be much greater than the rate of NO autooxidation,<sup>24–26</sup> especially when the NO concentration is in the submicromolar to low nanomolar range. As a result, Cygb may act to sense O<sub>2</sub> levels in the vascular wall and to regulate the NO decay rate and diffusion distance in response to changes in O<sub>2</sub> concentration.

Hargrove et al. suggested that heme globin (Hgb)-mediated NO dioxygenation is limited by the reduction of Hgb<sup>3+</sup> to Hgb<sup>2+</sup>, and the mechanism includes the following reaction cycle:<sup>8</sup>



However, subsequently, Gardner et al. reported that the rate of dioxygenation of NO by Cygb and Asc is much greater than that predicted from the rate constant for reduction of Cygb by Asc.<sup>10</sup> They suggested that Cygb(Fe<sup>3+</sup>) is not an obligate intermediate in the reaction cycle. Thus, it remains uncertain if the reaction cycle given above including Cygb(Fe<sup>3+</sup>) as an intermediate is valid or if other intermediates must be included. To evaluate the role of Cygb in the process of vascular NO decay, it is critically important to determine the precise reaction mechanism that underlies its O<sub>2</sub>-dependent NO metabolism.

In this study, we measure the O<sub>2</sub>-dependent rates of catabolism of NO by Cygb in the presence of the physiological reducing agent Asc, or the enzymatic reducing system CPR, using electrochemical and UV–vis spectroscopic methods. The molecular mechanism underlying O<sub>2</sub>-dependent Cygb-mediated NO consumption is elucidated and a kinetic model derived that serves to validate this mechanism and predict the rate of NO consumption for given levels of Cygb, O<sub>2</sub>, NO, and reductants. Our results reveal that the rate of Cygb-mediated NO dioxygenation is sufficient to provide O<sub>2</sub>-dependent regulation of NO levels in the vascular wall and serve as the major mechanism of NO decay.

## MATERIALS AND METHODS

### Expression and Purification of Recombinant Cygb.

The expression plasmid for Cygb (human Cygb cDNA in pET3a) was obtained from Thorsten Burmester (Mainz, Germany) and transformed into *Escherichia coli* strain BL21-(DE3)PLysS. Cells were grown in Terrific Broth (47.6 g/L) supplemented with glycerol (8 mL/L) and ampicillin (0.2 g/L) and chloramphenicol (0.1 g/L) in a total volume of 1 L in a 37 °C shaker. The cells were induced with IPTG at an A<sub>600</sub> between 0.6 and 0.8 OD. After induction, cells were grown overnight in a shaker at 25 °C. Cells were harvested by centrifugation and suspended in approximately 100 mL of 50 mM Tris-HCl (pH 7.5), 0.5 M NaCl, 1 mM EDTA, 5 mM dithiothreitol, and Roche complete protease inhibitor tablets. After cells had been suspended, approximately 0.1 volume of 10% Triton X-100, 10% deoxycholic acid, 500 mM Tris-HCl (pH 7.5), and 20 mM EDTA were added, and the cells were lysed by being passed through a high-pressure homogenizer (EmulsiFlex-C3 by AVESTIN, Inc., Ottawa, ON). The inclusion bodies were pelleted by centrifugation at 3300g for 15 min, and the pellet was resuspended and washed three times

in 1% Triton X-100, 50 mM Tris-HCl (pH 7.5), and 1 mM EDTA. Solubilization of the inclusion bodies was conducted in 6 M guanidinium hydrochloride, 100 mM NaCl, 0.1 mM EDTA, 50 mM Tris-HCl (pH 7.5), and 1% 2-mercaptoethanol for at least 1 h in a cold room at 4 °C. After solubilization, a 1.4-fold excess of hemin was added with very gentle stirring for 1 h prior to the solution being placed in dialysis tubing. The human Cygb was dialyzed against 50 mM Tris-HCl (pH 7.5), 100 mM NaCl, and 0.1 mM EDTA at 4 °C. After dialysis, insoluble material was removed by centrifugation (45000g for 1.5 h) and the human Cygb was concentrated using Amicon Ultra-15 centrifugal filters (Millipore Corp., Billerica, MA) with a 10000 molecular weight cutoff. Final purification was done on a GE Healthcare AKTA purifier system using a HiPrep 26/60 Sephacryl S-300 High Resolution size-exclusion column eluted with 50 mM Tris-HCl (pH 7.5), 100 mM NaCl, and 0.1 mM EDTA. The protein was concentrated and stored in 50 μL aliquots in a –80 °C freezer.

### Experimental Setup for Measurements of NO Concentration, O<sub>2</sub> Concentration, and UV–Vis Spectra of Cygb.

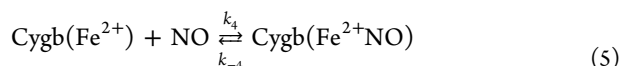
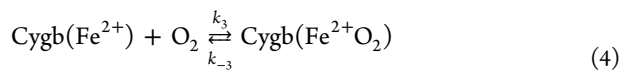
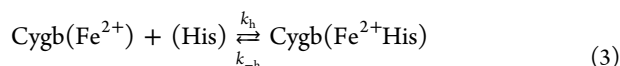
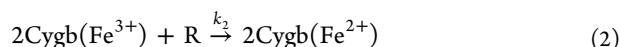
The measurements were performed in a four-port water-jacketed electrochemical chamber (NOCHM-4 from WPI, Sarasota, FL) containing 1.5 or 2 mL of Dulbecco's phosphate-buffered saline [DPBS (pH 7.0)] (Thermo Scientific, South Logan, UT) at 37 °C.<sup>26,27</sup> The solution was rapidly stirred with a magnetic stirring bar during the NO and O<sub>2</sub> measurements. A NO electrode and an O<sub>2</sub> electrode (WPI) were placed in the chamber through two ports on the side wall of the electrochemical chamber. The two electrodes were connected to an Apollo 4000 electrochemical instrument (WPI). The NO solution was prepared as described previously.<sup>17,27</sup> After the electrodes had stabilized, NO (≤0.5 μM) was injected into the aerated buffer solution (under room air) in the absence of Cygb and reductants. When the NO concentration decreased to baseline, Cygb (≤0.8 μM), Asc or CPR (a gift from L. Waskell, University of Michigan, Ann Arbor, MI) with NADPH, and SOD were added to the chamber followed by injections of NO into the solution to measure the rate of NO consumption in room air. To measure the rate of consumption of NO by Cygb at different O<sub>2</sub> concentrations (≤200 μM), argon gas was introduced into the chamber headspace to remove O<sub>2</sub> from the solution. While the O<sub>2</sub> concentration was gradually decreased by the flow of argon gas, equal amounts of NO were repeatedly injected into the solution. Changes in O<sub>2</sub> concentration and NO concentration over time were recorded by the O<sub>2</sub> and NO electrodes, respectively. From the recorded temporal NO and O<sub>2</sub> concentration curves, the O<sub>2</sub> concentration and the rate of NO decay at each NO peak were determined. In preliminary experiments measuring the rate of NO decay, we observed that Asc or CPR/NADPH alone could increase the NO consumption rate secondary to the superoxide generation that occurs in the presence of these reductants. However, SOD concentrations of 400 units/mL were sufficient to scavenge the superoxide produced and abolish any increase in the rate of consumption of NO from Asc or CPR/NADPH alone. Therefore, 400 units/mL SOD was included in all aerobic experiments.

### Reduction of Cygb(Fe<sup>3+</sup>) by Asc and by CPR/NADPH.

The reduction of Cygb(Fe<sup>3+</sup>) by Asc or CPR/NADPH was measured in a cuvette with a Cary 50 UV–vis spectrophotometer (Varian, Inc., Palo Alto, CA) under anaerobic conditions at 37 °C. The buffer solution in the cuvette was deaerated by bubbling argon gas into the solution in the

presence of NADPH (for reduction of Cygb by CPR/NADPH) or in the absence of NADPH (for reduction of Cygb by Asc) for at least 15 min. After 10  $\mu\text{M}$  deaerated  $\text{Cygb}(\text{Fe}^{3+})$  had been added to the chamber, the tube was moved to the gas phase above the solution surface and the argon gas flow was maintained in the chamber during the experiments. After 15 min, a certain amount of deaerated Asc or CPR was then injected into the chamber to start the reduction. Gastight syringes were used for the injections of these samples. The syringes were inserted into a tube with flowing argon, and the syringes were drawn and pushed several times to remove any remaining  $\text{O}_2$  in the syringes before sampling. The reduction was monitored by scanning the wavelength from 350 to 700 nm or by recording the absorbance change at the absorbance peak of the corresponding Soret band.

**Mathematical Model of the  $\text{O}_2$ -Dependent Consumption of NO by Cygb.** The  $\text{O}_2$ -regulated NO consumption by Cygb can be expressed by the following reaction equations based on similar mechanisms for flavohemoglobin<sup>28</sup> and neuroglobin:<sup>21</sup>



where R is Asc or CPR. The rate of NO consumption in eq 1 can be written as

$$V_{\text{NO}} = k_1[\text{Cygb}(\text{Fe}^{2+}\text{O}_2)][\text{NO}] \quad (6)$$

Using the steady-state approximation approach, the rate equation for consumption of NO by Cygb is as follows:

$$V_{\text{NO}} = \left( k_1[\text{E}][\text{NO}][\text{O}_2] \right) / \left( [\text{O}_2] \left( 1 + \frac{k_1[\text{NO}]}{k_2[\text{R}]} \right) + \left( \frac{k_{-3}}{k_3} + \frac{k_1}{k_3}[\text{NO}] \right) \left( 1 + \frac{k_4}{k_{-4}}[\text{NO}] + \frac{k_h}{k_{-h}} \right) \right) \quad (7)$$

where [E] is the total Cygb concentration. Concentrations of each Cygb species as a function of  $\text{O}_2$  concentration are as follows:

$$[\text{Cygb}(\text{Fe}^{2+})] = [\text{E}] / \left( 1 + \frac{k_4[\text{NO}]}{k_{-4}} + \frac{k_h}{k_{-h}} + \left( 1 + \frac{k_1[\text{NO}]}{k_2[\text{R}]} \right) \frac{k_3[\text{O}_2]}{k_{-3} + k_1[\text{NO}]} \right) \quad (8)$$

$$[\text{Cygb}(\text{Fe}^{2+}\text{O}_2)] = \frac{k_3[\text{Cygb}(\text{Fe}^{2+})][\text{O}_2]}{k_{-3} + k_1[\text{NO}]} \quad (9)$$

$$[\text{Cygb}(\text{Fe}^{3+})] = \frac{k_1 k_3 [\text{Cygb}(\text{Fe}^{2+})][\text{O}_2][\text{NO}]}{k_2[\text{R}](k_{-3} + k_1[\text{NO}])} \quad (10)$$

$$[\text{Cygb}(\text{Fe}^{2+}\text{NO})] = \frac{k_4[\text{Cygb}(\text{Fe}^{2+})][\text{NO}]}{k_{-4}} \quad (11)$$

$$[\text{Cygb}(\text{Fe}^{2+}\text{His})] = \frac{k_h[\text{Cygb}(\text{Fe}^{2+})]}{k_{-h}} \quad (12)$$

Equation 7 can be arranged in an apparent Michaelis–Menten form:

$$V_{\text{NO}} = \frac{V_{\text{m}}[\text{O}_2]}{K_{\text{m}} + [\text{O}_2]} \quad (13)$$

where

$$V_{\text{max}} = \frac{k_1 k_2 [\text{R}][\text{E}][\text{NO}]}{k_2[\text{R}] + k_1[\text{NO}]} \quad (14)$$

$$K_{\text{m}} = \left[ k_2[\text{R}] \left( \frac{k_{-3}}{k_3} + \frac{k_1}{k_3}[\text{NO}] \right) \left( 1 + \frac{k_h}{k_{-h}} + \frac{k_4}{k_{-4}}[\text{NO}] \right) \right] / \left( k_2[\text{R}] + k_1[\text{NO}] \right) \quad (15)$$

Because NO decay in these experiments is not only caused by Cygb-mediated NO consumption but also caused by NO autoxidation in the presence of  $\text{O}_2$  and by diffusion out of solution, the measured total NO decay rate ( $V_{\text{total}}$ ) should be expressed as follows:

$$V_{\text{total}} = V_{\text{NO}} + V_{\text{d}} + k_{\text{au}}[\text{O}_2][\text{NO}]^2 \quad (16)$$

where  $V_{\text{d}}$  is the rate of diffusion of NO from the solution and  $k_{\text{au}}$  is the rate constant of NO autoxidation. In data analysis and figures, we use  $V_{\text{Cygb-NO}}$  to represent  $V_{\text{total}} - V_{\text{d}}$ :

$$V_{\text{Cygb-NO}} = V_{\text{total}} - V_{\text{d}} = V_{\text{NO}} + V_{\text{au}} \quad (17)$$

where  $V_{\text{au}}$  is the rate of NO autoxidation.

## RESULTS

**Effect of  $\text{O}_2$  Concentration on the Rate of Consumption of NO by Cygb.** To measure the rate of consumption of NO by Cygb in the presence of Asc or in the presence of CPR/NADPH at different  $\text{O}_2$  concentrations, simultaneous recording of NO and  $\text{O}_2$  concentration changes was performed. A pair of such experimental curves is shown in Figure 1, in which 0.5  $\mu\text{M}$  NO was repeatedly added to the solution (initial  $[\text{O}_2] = 200 \mu\text{M}$ ) containing 0.4  $\mu\text{M}$  Cygb, 300  $\mu\text{M}$  Asc, and 400 units/mL SOD. Argon gas flow was started above the solution at the time designated by the upward arrow to slowly remove  $\text{O}_2$  from the solution. The curves of NO decay in the presence of Cygb, Asc, and SOD at different  $\text{O}_2$  concentrations are shown in Figure 1A (solid line). A curve of NO decay in the aerated buffer solution without proteins and reductants is shown in Figure 1A (dashed line) at the right end to compare with the last NO decay curve under anaerobic conditions. The initial rate of consumption of NO by Cygb for each injection of NO was measured from a segment of the curve immediately following each NO peak using the formula  $V_{\text{total}} = \Delta c / \Delta t$ . The rate of diffusion of NO from the solution ( $V_{\text{d}}$ ) was considered to be approximately equal to the  $V_{\text{total}}$  of



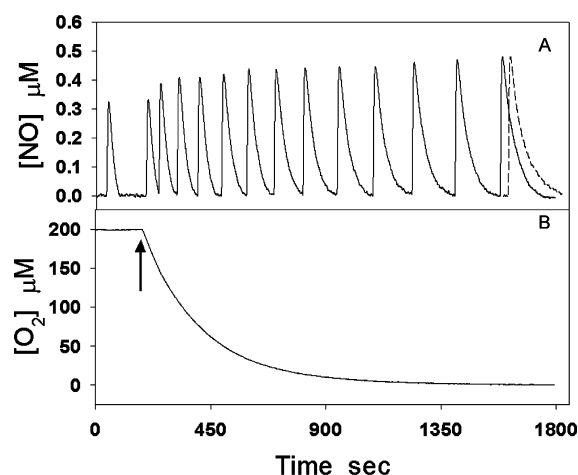


**Figure 1.** Measurements of rates of consumption of NO by Cygb and cellular reductants at varying  $O_2$  concentrations. (A) NO ( $0.5 \mu M$ ) was repeatedly added to the solution containing  $0.4 \mu M$  Cygb,  $300 \mu M$  Asc, and  $400$  units/mL SOD. The dashed curve was recorded after injection of  $0.5 \mu M$  NO into the aerated solution in the absence of Asc, SOD, and Cygb under room air. (B) The solution was initially aerated with  $200 \mu M O_2$ , and then the argon gas flow started above the solution (see Materials and Methods) at the time designated by the arrow to slowly remove  $O_2$  from the solution.

the rate for the last NO decay curve (the solid curve at the right end in Figure 1A) under anaerobic conditions.  $V_d$  was subtracted from  $V_{total}$  yielding  $V_{Cyto-NO}$ . The corresponding  $O_2$  concentrations were read at the time of each NO peak. The rate of consumption of NO by Cygb was found to decrease with a decreasing  $O_2$  concentration with either Asc (the top curve in Figure 1) or CPR/NADPH (not shown) as a reductant. A plot of the  $O_2$  concentration dependence of the initial rate of consumption of NO by Cygb in the presence of  $300 \mu M$  Asc and  $400$  units/mL SOD or  $400 \mu M$  NADPH,  $50$  nM CPR, and  $400$  units/mL SOD (●) (Figure 2) shows that the NO consumption rate is hyperbolic with respect to  $O_2$  concentration, with an only modest decline above  $50 \mu M O_2$  but a much steeper drop at lower  $O_2$  concentrations.

**Reduction of metCygb by Asc and by CPR/NADPH.** A change in the UV-vis spectrum characteristic of the reduction of metCygb is seen following addition of Asc or CPR with NADPH under anaerobic conditions (Figure 3A,B). The inset

of Figure 3A shows spectra for the complete reduction of metCygb (solid line) into ferrous Cygb (dashed line) with an excess of dithionite under anaerobic conditions. Panels A and B of Figure 3 demonstrate the reduction process of metCygb that was recorded at  $416$  nm to monitor the decrease in metCygb concentration after the reduction was initiated by  $10$  mM Asc or  $50$  nM CPR with  $400 \mu M$  NADPH. SOD was not included in these anaerobic experiments because  $O_2$ , the source of superoxide, was not present. To characterize the kinetics of metCygb reduction as a function of the level of the cellular reductant Asc, we measured the initial rate of reduction of  $10 \mu M$  metCygb in the presence of different Asc concentrations ( $0.1$ – $40$  mM) using the following approximate equation:

$$V_{Cygb} \approx \alpha \frac{\Delta A}{\Delta t} = \frac{\Delta c}{\Delta t} \quad (18)$$

where  $\Delta A$  and  $\Delta t$  are the initial changes in absorbance and time, respectively,  $\Delta c$  is the initial change in metCygb concentration, and  $\alpha$  is the conversion factor to convert the change in absorbance at  $416$  nm into the concentration change, which was obtained from the inset of Figure 3A. It was observed that  $V_{Cygb}$  is not linear with  $[R]$  for values of  $[R]$  exceeding  $10$  mM (Figure 3C). The plot of  $V_{Cygb}$  versus  $[Asc]$  was very well fitted by the Michaelis–Menten equation with a  $K_m'$  of  $4.1 \pm 0.5$  mM and a  $V_{max}'$  of  $1.48 \pm 0.05 \mu M/s$  ( $n = 5$ ).

$$V_{Cygb} = \frac{V_{max}'[R]}{K_m' + [R]} \quad (19)$$

If  $[R]$  is far smaller than  $K_m'$ , the rate of reduction of metCygb by Asc can be approximately expressed as

$$\begin{aligned} V_{Cygb} &= \frac{V_{max}'[R]}{K_m' + [R]} \\ &= \frac{k_{cat}}{K_m' + [R]} [\text{metCygb}]_0 [R] \\ &\approx \frac{k_{cat}}{K_m'} [\text{Cygb}]_0 [R] \\ &= k_{ca} [\text{metCygb}]_0 [R] \end{aligned} \quad (20)$$

In the experiments that examine the reduction of metCygb by Asc,  $[\text{metCygb}]_0 = 10 \mu M$ . From eq 20, we determined the apparent second-order rate constant of reduction of metCygb

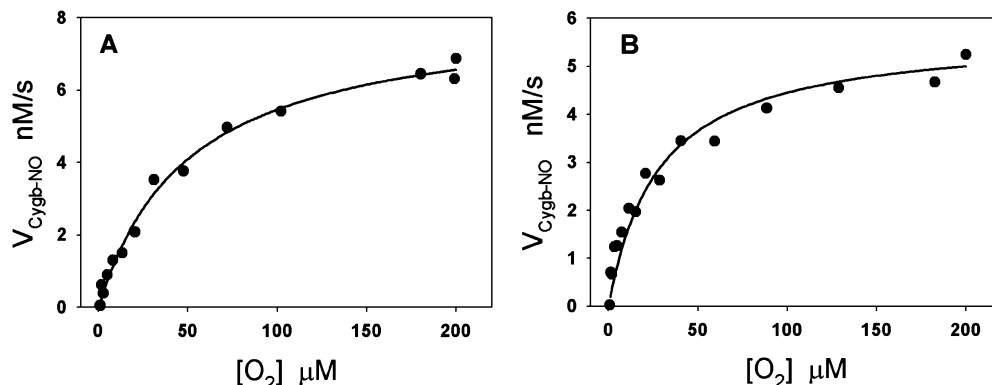


**Figure 2.** Oxygen-dependent rate of consumption of NO by Cygb with Asc or CPR/NADPH as the reductant. The data points (●) were obtained by repeatedly adding  $0.5 \mu M$  NO to a solution containing  $0.4 \mu M$  Cygb,  $300 \mu M$  Asc, and  $400$  units/mL SOD (A) or  $0.4 \mu M$  NO to a solution containing  $0.3 \mu M$  Cygb,  $400$  units/mL SOD,  $50$  nM CPR, and  $400 \mu M$  NADPH (B). The solid lines are fitted curves to the experimental data points.

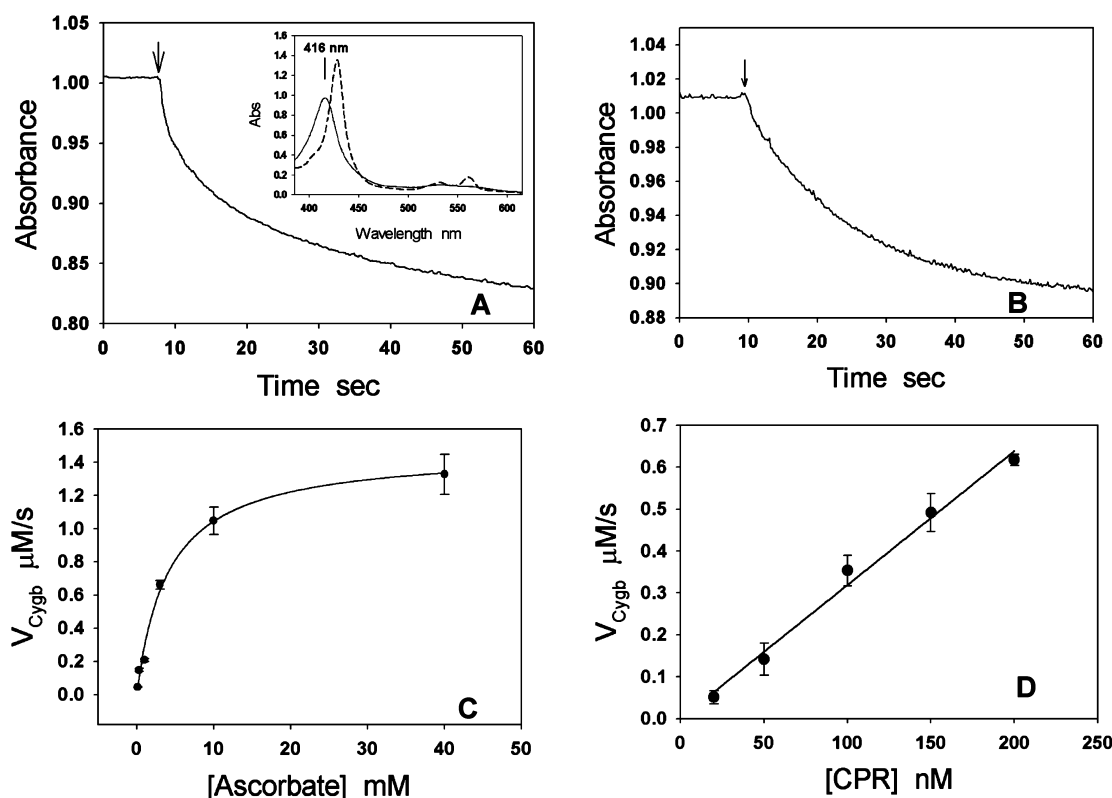


**Figure 3.** Reduction of metCygb by Asc and CPR/NADPH under anaerobic conditions at 37 °C. (A and B) Change in absorbance at 416 nm after 10 mM Asc had been added (designated by the arrow) to the solution containing 10  $\mu\text{M}$  metCygb (A) or 50 nM CPR had been added (designated by the arrow) to the solution containing 10  $\mu\text{M}$  metCygb and 400  $\mu\text{M}$  NADPH (B). The complete reduction of metCygb to ferrous Cygb by dithionite under anaerobic conditions is shown in the inset of panel A. (C) From a series of experiments similar to that shown in panel A with varying ascorbate concentrations, the initial rate of metCygb reduction ( $V_{\text{Cygb}}$ ) vs Asc concentration was plotted and found to follow apparent Michaelis–Menten kinetic behavior with a  $K_m'$  of  $4.1 \pm 0.5$  mM and a  $V_{\text{max}}'$  of  $1.48 \pm 0.05$   $\mu\text{M/s}$  ( $n = 5$ ). The apparent second-order rate constant for reduction of metCygb by Asc ( $k_2$  for Asc as the reductant or  $k_{\text{ca}}$ ) was determined from eq 20 to be  $36.1 \pm 4.4$   $\text{M}^{-1} \text{s}^{-1}$ . (D) In contrast, a series of experiments similar to those depicted in panel B with varying CPR concentrations show that the rate of reduction of metCygb by CPR/NADPH is linear with CPR concentration ( $n = 4$ ). The second-order rate constant for reduction of metCygb by CPR with NADPH ( $k_2$ ) is determined to be  $(3.2 \pm 0.1) \times 10^5$   $\text{M}^{-1} \text{s}^{-1}$ . Rates of metCygb reduction were measured from changes in absorbance (A and B) using the equation  $V_{\text{Cygb}} = \alpha dA/dt \approx \alpha \Delta A/\Delta t$ , where  $\alpha = 1/(\epsilon_1 - \epsilon_2) = 26$  and  $\epsilon_1$  and  $\epsilon_2$  are extinction coefficients of 1  $\mu\text{M}$  metCygb and 1  $\mu\text{M}$  deoxyCygb at 416 nm, respectively.

by Asc ( $k_2$  for Asc as the reductant or  $k_{\text{ca}}$ ) and obtained a value of  $36.1 \pm 4.4$   $\text{M}^{-1} \text{s}^{-1}$ .

The rate of reduction of metCygb by CPR with 400  $\mu\text{M}$  NADPH is linear with CPR concentration in the concentration range tested ( $20 \text{ nM} \leq [\text{CPR}] \leq 200 \text{ nM}$ ). The plot of  $V_{\text{Cygb}}$  versus CPR concentration is shown in Figure 3D. The second-order rate constant  $k_2$  for CPR/NADPH as the reductant or  $k_{\text{cnp}}$  can be calculated from the slope of the line, which is  $(3.2 \pm 0.2) \times 10^5$   $\text{M}^{-1} \text{s}^{-1}$  ( $n = 3$ ).

**Computer Simulations of Consumption of NO by Cygb.** Using the rate constants reported in the literature and measured in our experiments (Table 1), we performed computer simulations of the  $\text{O}_2$ -dependent consumption of NO by Cygb in the presence of Asc using eq 17 with eq 7. Experimental parameters in the equation, such as Cygb concentration  $[\text{E}]$ , Asc concentration  $[\text{R}]$ ,  $\text{O}_2$  concentration  $[\text{O}_2]$ , and NO concentration  $[\text{NO}]$ , were the same as the values used in the experiments shown in Figures 1 and 2.

Because the experiments were performed at 37 °C, the computer simulations require rate constants and equilibrium constants obtained at 37 °C; however, some of these constants are not available in the literature. In this case, the values of these parameters at 37 °C were calculated or estimated from available data. The reported  $k_1$  for Cygb at 20 °C is  $2.2 \times 10^7$

$\text{M}^{-1} \text{s}^{-1}$ .<sup>8</sup> For comparison, it is known that  $k_1$  for Mb ranges from  $3.1 \times 10^7$  to  $3.7 \times 10^7$   $\text{M}^{-1} \text{s}^{-1}$  in the temperature range of 10–25 °C.<sup>29–31</sup> Assuming that the temperature dependencies of  $k_1$  for Cygb and Mb are similar, we used a  $k_1$  of  $3 \times 10^7$   $\text{M}^{-1} \text{s}^{-1}$  for Cygb at 37 °C. The  $k_2$  rate constants were measured in our experiments as  $k_{\text{cnp}}$  for the Cygb/NADPH/CPR reaction system or  $k_{\text{ca}}$  for the Cygb/Asc reaction system. The reported values of  $k_3$  ( $k_{\text{on}}$ ) and  $k_{-3}$  ( $k_{\text{off}}$ ) at 25 °C for Cygb of the pentacoordinated form are  $2.5\text{--}2.7 \times 10^7$   $\text{M}^{-1} \text{s}^{-1}$  and  $0.9$   $\text{s}^{-1}$ , respectively.<sup>22,32</sup> The activation energy of  $k_3$  is between 8 and 10.5 kcal/mol, and the activation energy of  $k_{-3}$  is between 23 and 25.5 kcal/mol.<sup>33</sup> Using these activation energies and reported values of  $k_3$  and  $k_{-3}$  at 25 °C, we calculated  $k_3$  and  $k_{-3}$  at 37 °C to be  $3.5 \times 10^7$   $\text{M}^{-1} \text{s}^{-1}$  and  $1.3$   $\text{s}^{-1}$ , respectively. The  $\text{O}_2$  dissociation constant  $K_{3d}$  can be calculated from the ratio of  $k_{-3}$  to  $k_3$  ( $K_{3d} = k_{-3}/k_3 = 37$  nM).  $K_{3d}$  is the intrinsic  $\text{O}_2$  dissociation constant of the pentacoordinated form rather than the hexacoordinated form. The observed  $\text{O}_2$  dissociation constant ( $K_{3d}^{\text{obs}}$ ) of the hexacoordinated Cygb depends on the competition between  $\text{O}_2$  and the endogenous sixth ligand following the equation  $K_{3d}^{\text{obs}} = K_{3d}(1 + K_H)$ , where  $K_H = k_h/k_{-h}$  is the association constant of the endogenous sixth ligand. Using values of  $k_h$  and  $k_{-h}$  ( $k_h/k_{-h} = 140$ ) at 25 °C<sup>22</sup> and the difference in activation energies ( $E_a^{\text{on}} - E_a^{\text{off}}$ ) for histidine

**Table 1.** Kinetic and Equilibrium Constants for Cygb<sup>a</sup>

parameter	value	ref
$k_1$	$2.2 \times 10^7 \text{ M}^{-1} \text{ s}^{-1}$ (20 °C)	8
	$3 \times 10^7 \text{ M}^{-1} \text{ s}^{-1}$ (37 °C)	estimated
$k_2$ ( $k_{\text{cnp}}$ or $k_{\text{ca}}$ )	<b><math>36.1</math> (56) <math>\text{M}^{-1} \text{ s}^{-1}</math></b> (37 °C) (by Asc)	this work
	<b><math>3.2 \times 10^5</math> (<math>3.5 \times 10^5</math>) <math>\text{M}^{-1} \text{ s}^{-1}</math></b> (37 °C) (by CPR/NADPH)	
$k_{-3}/k_3$	35 nM (25 °C)	22
	<b>37 nM</b> (37 °C)	calculated
$k_{-3}$	0.9 $\text{s}^{-1}$ (25 °C)	32
	<b>1.3 <math>\text{s}^{-1}</math></b> (37 °C)	calculated
$k_3$	$2.5 \times 10^7 \text{ M}^{-1} \text{ s}^{-1}$ (25 °C)	22
	$2.7 \times 10^7 \text{ M}^{-1} \text{ s}^{-1}$ (25 °C)	32
	<b><math>3.5 \times 10^7 \text{ M}^{-1} \text{ s}^{-1}</math></b> (37 °C)	calculated
$k_h/k_{-h}$	140 (25 °C)	22
	<b>165</b> (37 °C)	calculated
$k_{-4}/k_4$	8 pM (37 °C)	estimated
$k_{\text{au}}$	<b><math>11 \times 10^6 \text{ M}^{-2} \text{ s}^{-1}</math></b> (37 °C)	27

<sup>a</sup>The values of rate constant  $k_2$  of  $36.1 \text{ M}^{-1} \text{ s}^{-1}$  (Asc) and  $3.2 \times 10^5 \text{ M}^{-1} \text{ s}^{-1}$  (CPR/NADPH) were obtained experimentally, and the values of rate constant  $k_2$  of 56 and  $3.5 \times 10^5 \text{ M}^{-1} \text{ s}^{-1}$  were obtained from computer simulations. Experimentally measured values of parameters at 20 or 25 °C appear in lightface, while the values of parameters at 37 °C (calculated, estimated, or from literature) appear in boldface.

binding that are between 8 and 13 kcal/mol,<sup>33</sup> we calculated a value of 165 for the association constant of the endogenous sixth ligand ( $K_H = k_h/k_{-h}$ ) at 37 °C. If  $K_{3d}$  is 37 nM and  $K_H$  is 165, the calculated  $K_{3d}^{\text{obs}}$  is 6.1  $\mu\text{M}$ , which is close to the reported  $P_{50}$  of Cygb at 37 °C.<sup>34</sup> For rate constants  $k_4$  and  $k_{-4}$ , we could not find the available values for Cygb at any temperature in the literature. However, it has been reported that the equilibrium dissociation constant ( $k_{-4}/k_4$ ) of three other globins (Ngb, Hb, and Mb) is in the range of 1–8 pM at 20–25 °C.<sup>28,35–37</sup> A higher range for  $k_{-4}/k_4$  should be seen when the temperature is increased to 37 °C because the equilibrium dissociation constant increases with temperature. Therefore, we assumed that the equilibrium dissociation constant of Cygb at 37 °C is in the range of a few picomolar or slightly higher than 10 pM. The simulated curve of  $V_{\text{Cygb-NO}}$  versus  $[\text{O}_2]$  is shown in Figure 4. In the simulation, we let the value of  $k_2$  float to best fit the experimental data, and it was

found that the simulated curve closely fits the experimental data when  $k_2$  is  $56 \text{ M}^{-1} \text{ s}^{-1}$  (Figure 4A) when Asc is the reductant and  $3.5 \times 10^5 \text{ M}^{-1} \text{ s}^{-1}$  (Figure 4B) when CPR (with 400  $\mu\text{M}$  NADPH) is the reductant, 1.55 times the  $k_{\text{ca}}$  value and 1.09 times the  $k_{\text{cnp}}$  value measured in our experiments, respectively. Final parameters used in the simulated curve are listed (boldface) in Table 1.

**Effect of Concentrations of Asc, NO, and Cygb on the Rate of O<sub>2</sub>-Dependent Consumption of NO by Cygb in the Presence of Asc.** Equation 7 can be rearranged in Michaelis–Menten form (eqs 13–15). Equation 7 shows that  $V_{\text{Cygb-NO}}$  is linear with Cygb concentration  $[\text{E}]$ , while eqs 14 and 15 show that both  $V_{\text{max}}$  and  $K_m$  are a function of  $[\text{NO}]$  and  $[\text{R}]$ . To test eq 7, we substituted eq 7 into eq 17 and used eq 17 to simulate the effect of the concentrations of Asc (Figure 5A), NO (Figure 5B), and Cygb (Figure 5C) on the O<sub>2</sub>-dependent rate of consumption of NO by Cygb and compared these results to the related experimental data. The calculated curves from eq 17 are in good agreement with the experimental data.

**Effect of O<sub>2</sub> on the Concentrations of Different Cygb Species.** The mathematical model was used to further examine the O<sub>2</sub> concentration dependence of each Cygb species for a reducing system with 300  $\mu\text{M}$  Asc in the presence of 0.4  $\mu\text{M}$  Cygb with 0.5  $\mu\text{M}$  NO, which are the same or close to the concentrations used in the experiments. The simulated concentrations of Cygb( $\text{Fe}^{3+}$ ), Cygb( $\text{Fe}^{2+}\text{NO}$ ), and Cygb( $\text{Fe}^{2+}\text{O}_2$ ) are shown in panels A and B of Figure 6. The concentrations of Cygb( $\text{Fe}^{3+}$ ), Cygb( $\text{Fe}^{2+}\text{NO}$ ), and Cygb( $\text{Fe}^{2+}\text{O}_2$ ) were seen to greatly change with O<sub>2</sub> concentration. Because the rate of dioxygenation of NO by Cygb is proportional to Cygb( $\text{Fe}^{2+}\text{O}_2$ ) concentration, this indicates that changes in O<sub>2</sub> concentration can greatly regulate the rate of NO consumption.

## DISCUSSION

It has been observed that the rate of consumption of NO by cells is O<sub>2</sub>-dependent.<sup>17,38</sup> Computer simulation demonstrated that the O<sub>2</sub>-dependent NO consumption can significantly change the NO diffusion distance in the intervacular tissue.<sup>17</sup> Experimental data and mathematical modeling have further demonstrated that O<sub>2</sub>-dependent NO consumption in the vascular wall can act as an O<sub>2</sub> sensor to change the NO diffusion distance in the vascular wall.<sup>16,39</sup> Recent evidence has

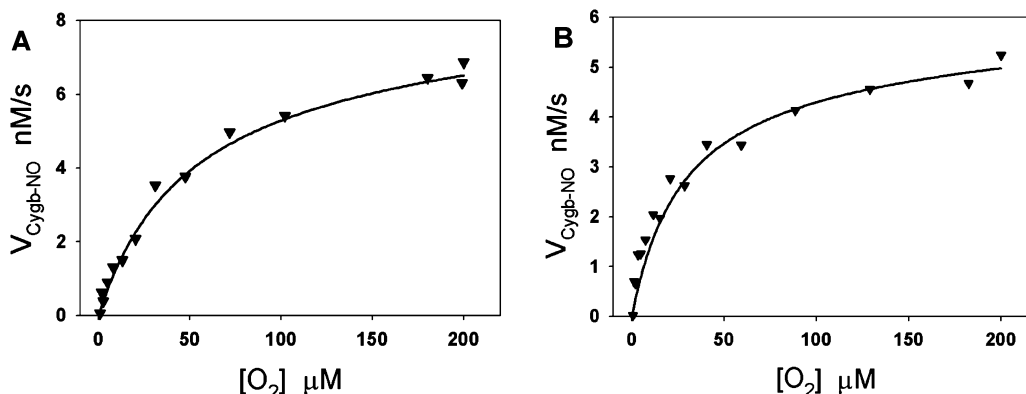


**Figure 4.** Simulations of experimental data using eqs 7 and 17. (A and B) Rate of O<sub>2</sub>-dependent NO consumption (▼) mediated by 0.4  $\mu\text{M}$  Cygb in the presence of 300  $\mu\text{M}$  Asc and 400 units/mL SOD (A) and by 0.3  $\mu\text{M}$  Cygb in the presence of 50 nM CPR, 400  $\mu\text{M}$  NADPH, and 400 units/mL SOD (B). The solid lines in panels A and B are simulated curves from eqs 7 and 17 assuming the  $k_2$  for Asc is  $56 \text{ M}^{-1} \text{ s}^{-1}$  and the  $k_2$  for CPR/NADPH is  $3.5 \times 10^5 \text{ M}^{-1} \text{ s}^{-1}$ , respectively.

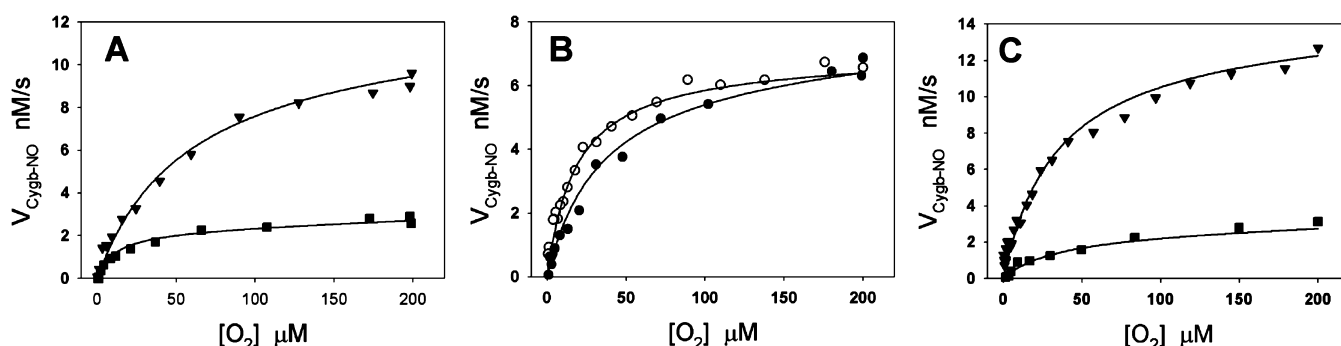


**Figure 5.** Effect of Asc concentration, NO concentration, and Cygb concentration on the  $O_2$ -dependent consumption of NO by Cygb. (A) Rate of consumption of 0.5  $\mu\text{M}$  NO in a solution containing 0.4  $\mu\text{M}$  Cygb, 400 units/mL SOD, and 100  $\mu\text{M}$  (■) or 500  $\mu\text{M}$  Asc (▼). (B) Rate of consumption of 0.25  $\mu\text{M}$  (○) or 0.5  $\mu\text{M}$  NO (●) in a solution containing 0.4  $\mu\text{M}$  Cygb, 400 units/mL SOD, and 300  $\mu\text{M}$  Asc. (C) Rate of consumption of 0.5  $\mu\text{M}$  NO in a solution containing 300  $\mu\text{M}$  Asc, 400 units/mL SOD, and 150 nM (■) or 800 nM Cygb (▼).

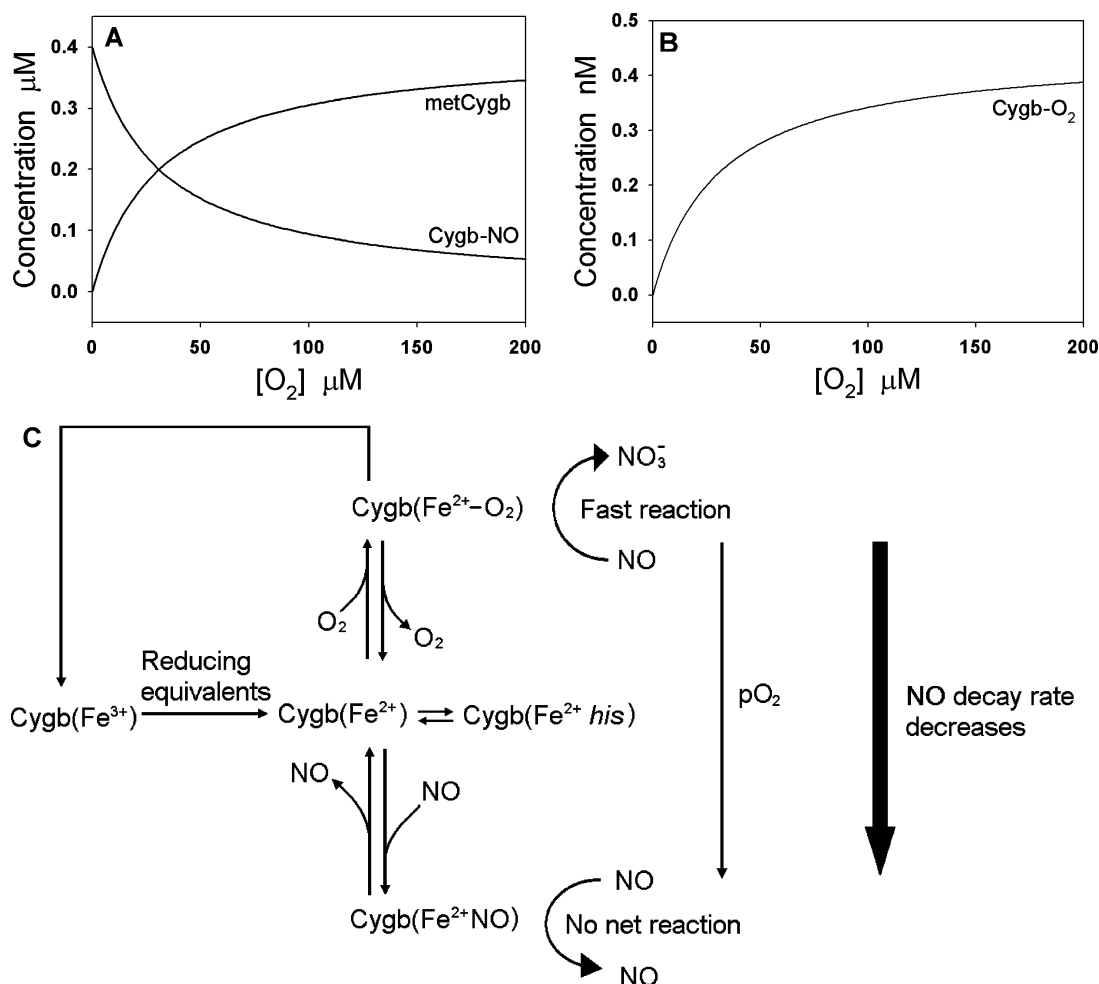


**Figure 6.** (A and B) Effect of  $O_2$  concentration on Cygb species and the proposed reaction scheme for reduction of Cygb. Simulated concentration changes of  $\text{Cygb(Fe}^{3+})$  and  $\text{Cygb(Fe}^{2+}\text{NO)}$  (A) and simulated concentration changes of  $\text{Cygb(Fe}^{2+}\text{O}_2)$  (B) when  $[O_2]$  varies from 0 to 200  $\mu\text{M}$  in a reaction system containing 300  $\mu\text{M}$  Asc, 0.4  $\mu\text{M}$  Cygb, and 0.5  $\mu\text{M}$  NO. (C) Molecular reaction mechanism of Cygb-mediated  $O_2$ -dependent NO consumption in response to hypoxia.

shown that Cygb is expressed in vascular smooth muscle (VSM),<sup>9</sup> a type of muscle lacking myoglobin.<sup>40</sup>

Cygb has been studied as an NO dioxygenase. It is interesting to consider why there is a need for a low concentration of NO dioxygenase with the properties of Cygb in vascular smooth muscle. A reasonable explanation may be that the presence of Cygb in this tissue is not simply for

metabolism of excess NO but specifically for the regulation of NO levels and decay kinetics required for signal transduction through soluble guanylate cyclase (sGC) in the vascular wall. In addition, because Cygb consumes NO in an  $O_2$ -dependent manner, this further imparts Cygb with the important function of regulating the vascular levels and kinetics of NO in response to changes in  $O_2$  concentration. Under hypoxic conditions, the



rate of decay of NO by Cygb is markedly decreased, and this could serve to support hypoxic vasodilation.

The Cygb concentration in the vascular wall has not been reported, but its concentrations in cells and tissues were measured or estimated to be in the range of  $\sim 1 \mu\text{M}$ .<sup>8,10,21–23</sup> Asc is an important cellular antioxidant that is a key vitamin for animals and plants. Asc concentrations are in the range of tens of micromolar in human serum,<sup>41–43</sup>  $\sim 300 \mu\text{M}$  in rat liver and brain cells,<sup>44</sup>  $0.5\text{--}1 \text{ mM}$  in human fibroblasts and endothelium,<sup>45,46</sup> and  $\sim 0.1 \text{ mM}$  in vascular smooth muscle cells<sup>47</sup> in the presence of  $50 \mu\text{M}$  extracellular Asc. In our experiments, the Asc concentration used for measuring the rate of Cygb-mediated NO decay (NO dioxygenation) is  $300 \mu\text{M}$ , which is in the physiological intracellular concentration range. The flavoprotein CPR/NADPH is a ubiquitous enzyme in eukaryotic cells that is capable of supporting the activity of all known microsomal forms of CPR.<sup>48</sup> It was reported that the content of CPR represents  $\sim 0.1\%$  of the aortic microsomal protein<sup>49</sup> and that the aortic microsomal protein content is  $3.3 \text{ mg/g}$  of tissue.<sup>50</sup> Assuming that the density of the aorta is 1, the aortic microsomal protein content should be  $3.3 \text{ mg/mL}$  or  $3.3 \text{ g/L}$ . Because the CPR content is  $\sim 0.1\%$  of the aortic microsomal protein, the CPR content should be  $\sim 3.3 \text{ mg/L}$ . The apparent molecular mass of CPR is  $\sim 80 \text{ kDa}$ , so its concentration in the aortic wall is estimated to be  $\sim 40 \text{ nM}$ . We used  $50 \text{ nM}$  CPR in experiments for Cygb-mediated NO consumption close to the inferred aortic CPR concentration.

In Figure 1, we demonstrate that the rate of consumption of NO by Cygb decreases when the  $\text{O}_2$  concentration decreases. It is worth noting that the rate of NO decay in the aerated buffer under room air (dashed line) is similar to the rate of NO decay under anaerobic conditions [the last NO decay curve (solid line) on the right side of Figure 1A]. It is well-known that NO autoxidation is second-order with respect to NO concentration, and its half-life is inversely proportional to the initial NO concentration. Theoretically, the half-life of  $0.5 \mu\text{M}$  NO is longer than 10 min if NO decay is caused only by NO autoxidation. However, in our measurements, the solution is rapidly stirred to achieve a uniform distribution in the whole solution as quickly as possible so that the rapid Cygb-mediated NO decay can be accurately recorded. Because NO is a volatile gas and the rate of NO volatilization is dependent on the rate of stirring, increasing the stirring speed could increase the rate of NO volatilization. Under our experimental conditions, NO decay in the absence of Cygb or reductants was mainly caused by NO volatilization rather than NO autoxidation. The plots of Cygb-mediated NO consumption in the presence of a reductant versus  $\text{O}_2$  concentration (Figure 2) show that the rate of NO consumption,  $V_{\text{Cygb-NO}}$ , decreases only slightly when the  $\text{O}_2$  concentration decreases at higher  $\text{O}_2$  levels ( $>50 \mu\text{M}$ ). In contrast,  $V_{\text{Cygb-NO}}$  is much more sensitive to the change in  $\text{O}_2$  concentration for lower  $\text{O}_2$  levels ( $<50 \mu\text{M}$ ), indicating that the major effect of Cygb in modulating  $\text{O}_2$ -dependent NO consumption occurs in this hypoxic range.

The magnitude of the change in  $V_{\text{Cygb-NO}}$  is largely dependent on the rate of NO consumption at high  $\text{O}_2$  concentrations, and the rate of Cygb-mediated NO consumption is limited by the reduction of metCygb back to ferrous Cygb after oxyCygb is oxidized to metCygb during NO dioxygenation, as suggested previously.<sup>8,28</sup> It is interesting that ferric Cygb (metCygb) can be reduced by many cellular reductants at a rate significantly higher than the rate of reduction of ferric myoglobin (metMb) and ferric neuroglobin

(metNgb).<sup>10</sup> This allows Cygb to more sensitively regulate the rate of NO consumption in response to changes in  $\text{O}_2$  concentration than these other globins.

The CPR concentration used in these experiments is  $\sim 3\text{--}4$  orders of magnitude smaller than the Asc concentration, while  $k_{\text{cpr}}$  is  $\sim 4$  orders of magnitude greater than  $k_{\text{ca}}$  (Figure 3). However, as noted above, the Asc concentration (several hundred micromolar) is  $\sim 4$  orders of magnitude higher than the levels of CPR ( $10\text{--}40 \text{ nM}$ ) in the aortic wall (unpublished observations). Therefore, both Asc and CPR have a comparable ability to reduce Cygb in the vascular wall if these reductants can freely interact with Cygb. CPR is known to be present in most cells, including vascular smooth muscle. While CPR is primarily present attached to the endoplasmic reticulum membrane, there are also reports of its distribution in some cells throughout the cytoplasm.<sup>51</sup> Cytochrome *c* is a cytosolic protein and could come into contact with CPR attached to the cytosolic side of the endoplasmic reticulum membrane or in other locations in the cytoplasm. More recently, CPR has also been reported to be associated with the cytosolic side of the plasma membrane and thus could also come into contact with cytochrome *c*.<sup>52</sup> CPR is known to reduce a range of heme proteins other than  $\text{P}_{450}$ , including cytochrome *c* and myoglobin. We observe that CPR efficiently and rapidly reduces cytochrome *c*. The use of CPR/NADPH as an alternative pathway of cytochrome *c* reduction not only demonstrates that the kinetic model illustrated in Figure 6 is suitable for different cellular reductants but also further validates that  $\text{Cygb(Fe}^{3+})$  is the main intermediate reduced back to ferrous Cygb by cellular reductants in the process of  $\text{O}_2$ -dependent NO consumption.

It is interesting that Asc reduces metCygb with kinetics that follow the Michaelis–Menten equation with an apparent  $K_{\text{m}}$  of  $4.1 \pm 0.5 \text{ mM}$  and a  $V_{\text{max}}$  of  $1.48 \pm 0.05 \mu\text{M/s}$ . This implies that reduction of metCygb by Asc may occur through a Cygb–Asc intermediate or Cygb may have a binding site for Asc as previously suggested.<sup>10</sup> The rate constant of reduction of Cygb by Asc that we measured ( $36.1 \text{ M}^{-1} \text{ s}^{-1}$ ) was obtained by directly measuring the metCygb concentration in the reaction with Asc. This value is approximately 26 times greater than that reported from measurements of the rate of formation of Cygb–CO during the reduction of metCygb by Asc in the presence of CO.<sup>10</sup> The previously reported rate constant for reduction of metCygb by Asc, obtained by measuring the formation of  $\text{Cygb(Fe}^{2+}\text{-CO)}$  during the reduction of  $\text{Cygb(Fe}^{3+})$  by Asc, was  $1.3 \text{ M}^{-1} \text{ s}^{-1}$ . The dissociation of the endogenous ligand required for CO binding may be the main contributor to this slower rate. Equations 1–5 were used to derive eqs 7 and 17 for the rate of Cygb-mediated  $\text{O}_2$ -dependent NO consumption. The calculated  $V_{\text{Cygb-NO}}$  versus  $[\text{O}_2]$  curves based on eq 17 fit the experimental data with an adjusted  $k_2$  that is 1.55 times the measured value for Asc as the reductant or 1.09 times the measured value for CPR/NADPH as the reducing system (Figure 4), indicating that the proposed reaction scheme is reasonable.

To examine the effect of different factors on the rate of consumption of NO by Cygb, we rearranged eq 7 in an apparent Michaelis–Menten form (eq 13). In this form,  $V_{\text{m}}$  and  $K_{\text{m}}$  are functions of Asc concentration, NO concentration, and reaction rate constants. Cygb concentration  $[\text{E}]$  appears in only  $V_{\text{m}}$ , while  $[\text{NO}]$  and  $[\text{R}]$  appear in both  $V_{\text{m}}$  and  $K_{\text{m}}$ . Therefore, we can predict that a change in the value of  $[\text{E}]$  affects only  $V_{\text{m}}$ , while a change in  $[\text{NO}]$  and  $[\text{R}]$  will affect both  $V_{\text{m}}$  and  $K_{\text{m}}$ .

These predictions were validated by the experimental results shown in Figure 5.

The proposed molecular reaction scheme for this regulation is illustrated in schematic form in Figure 6C. The relatively higher rate of reduction of metCygb by Asc or CPR/NADPH greatly increases the amount of reduced Cygb. In the presence of a high O<sub>2</sub> concentration, the Cygb(Fe<sup>2+</sup>NO) concentration is quite low (Figure 6A), but the Cygb(Fe<sup>2+</sup>O<sub>2</sub>) concentration is quite high (Figure 6B) such that much more Cygb(Fe<sup>2+</sup>O<sub>2</sub>) is available for the dioxygenation cycle. This results in a large increase in the rate of NO consumption. With a decreasing O<sub>2</sub> concentration, NO will be more likely to bind to the ferrous Cygb. This process converts Cygb into the nitrosyl form [Cygb(Fe<sup>2+</sup>NO)] at lower O<sub>2</sub> concentrations, which greatly reduces the amount of metCygb that can be reduced to ferrous Cygb and form Cygb(Fe<sup>2+</sup>O<sub>2</sub>) for the dioxygenation cycle. Furthermore, the nitrosyl form has a much lower chemical activity in reacting with NO, resulting in a significant decrease in the rate of NO consumption. In this way, Cygb effectively amplifies the extent of the change in the rate of NO consumption when the O<sub>2</sub> concentration is varied under hypoxic conditions.

As shown above, Cygb mainly regulates the rate of NO consumption when [O<sub>2</sub>] is below 50 μM. This concentration is close to the O<sub>2</sub> concentration measured in microvasculature and used in prior related computer simulations.<sup>17</sup> Equation 7 shows that the rate of consumption of NO by Cygb is not linear with NO concentration and O<sub>2</sub> concentration, but we can estimate the apparent rate constant of the O<sub>2</sub>-dependent consumption of NO by Cygb in the vascular wall based on eq 7 if vascular O<sub>2</sub>, NO, Cygb, and Asc concentrations are known. Assuming that the NO concentration in the vascular wall is less than 150 nM,<sup>17,53–55</sup> the O<sub>2</sub> concentration is below 60 μM, the Cygb concentration is 1 μM, the Asc concentration is 100 μM, and other rate constants are the same as those listed in Table 1, we can calculate the apparent rate (*k*<sub>app</sub>) of consumption of NO by Cygb for given NO and O<sub>2</sub> concentrations in the range of 25–150 nM and 1–60 μM, respectively, using the following formula:

$$k_{\text{app}} = \frac{V_{\text{NO}}}{[\text{NO}][\text{O}_2]}$$

The calculated *k*<sub>app</sub> is a function of NO concentration and O<sub>2</sub> concentration. The average *k*<sub>app</sub> can be determined in the ranges of NO (25–150 nM) and O<sub>2</sub> (1–60 μM) concentrations considered, which is 3.5 × 10<sup>3</sup> M<sup>−1</sup> s<sup>−1</sup>. The average *k*<sub>app</sub> is close to the rate constant of 4 × 10<sup>3</sup> M<sup>−1</sup> s<sup>−1</sup> for vascular NO consumption reported in our prior paper<sup>16</sup> and in the range of rate constants estimated in other reports.<sup>17</sup> Our results suggest that the NO concentration is regulated not only in the intervascular tissues<sup>17</sup> but also in the vascular wall, with Cygb playing an important role in this latter process.

In conclusion, we delineated the reaction mechanism of O<sub>2</sub>-dependent consumption of NO by Cygb and derived a related kinetic model that predicts the NO consumption rate. The predicted rate of O<sub>2</sub>-dependent consumption of NO by Cygb was consistent with the experimentally measured values. We observed that the reduction of Cygb by Asc follows Michaelis–Menten kinetics and determined the *K*<sub>m</sub> and *V*<sub>max</sub> for this reaction. In addition, we measured the rate constant of reduction of Cygb by the important cellular reductase CPR. Simulations based on the kinetic model show that Cygb

efficiently regulates the O<sub>2</sub>-dependent NO consumption rate because of the rapid reduction of metCygb, which increases the NO catabolic rate at high O<sub>2</sub> concentrations, while NO binding to Cygb at lower O<sub>2</sub> concentrations significantly decreases the rate of NO consumption under hypoxia. Our results indicate that Cygb can sensitively transduce a change in O<sub>2</sub> concentration to a change in the rate of NO consumption, allowing Cygb to sense and regulate the NO diffusion distance in the vascular wall and vascular tone in local tissues in response to changes in O<sub>2</sub> concentration.

## AUTHOR INFORMATION

### Corresponding Author

\*X.L.: 473 W. 12th Ave., Columbus, OH 43210; phone, (614) 292-1305; fax, (614) 292-8778; e-mail, xiaoping.liu@osumc.edu. J.L.Z.: 473 W. 12th Ave., Columbus, OH 43210; phone, (614) 247-7788; fax, (614) 247-7845; e-mail, jay.zweier@osumc.edu.

### Funding

This work was supported by National Institutes of Health Grants HL063744, HL065608, and HL38324.

### Notes

The authors declare no competing financial interest.

## ACKNOWLEDGMENTS

We thank Dr. Thorsten Burmester (Mainz, Germany) for providing the expression plasmid for Cygb (human Cygb cDNA in pET3a) and Dr. Lucy Waskell (University of Michigan) for providing the CPR.

## ABBREVIATIONS

Cygb, cytoglobin; Hb, hemoglobin; Mb, myoglobin; metMb, ferric myoglobin; Ngb, neuroglobin; metNgb, ferric neuroglobin; CPR, cytochrome P<sub>450</sub> reductase; CPR/NADPH, CPR with nicotinamide adenine dinucleotide phosphate; Asc, ascorbate; NO, nitric oxide; CO, carbon monoxide.

## REFERENCES

- (1) Burmester, T., Ebner, B., Weich, B., and Hankeln, T. (2002) Cytoglobin: A novel globin type ubiquitously expressed in vertebrate tissues. *Mol. Biol. Evol.* 19, 416–421.
- (2) Kawada, N., Kristensen, D. B., Asahina, K., Nakatani, K., Minamiyama, Y., Seki, S., and Yoshizato, K. (2001) Characterization of a stellate cell activation-associated protein (STAP) with peroxidase activity found in rat hepatic stellate cells. *J. Biol. Chem.* 276, 25318–25323.
- (3) Trent, J. T., III, and Hargrove, M. S. (2002) A ubiquitously expressed human hexacoordinate hemoglobin. *J. Biol. Chem.* 277, 19538–19545.
- (4) Hankeln, T., Ebner, B., Fuchs, C., Gerlach, F., Haberkamp, M., Laufs, T. L., Roesner, A., Schmidt, M., Weich, B., Wystub, S., Saaler-Reinhardt, S., Reuss, S., Bolognesi, M., De Sanctis, D., Marden, M. C., Kiger, L., Moens, L., Dewilde, S., Nevo, E., Avivi, A., Weber, R. E., Fago, A., and Burmester, T. (2005) Neuroglobin and cytoglobin in search of their role in the vertebrate globin family. *J. Inorg. Biochem.* 99, 110–119.
- (5) Schmidt, M., Gerlach, F., Avivi, A., Laufs, T., Wystub, S., Simpson, J. C., Nevo, E., Saaler-Reinhardt, S., Reuss, S., Hankeln, T., and Burmester, T. (2004) Cytoglobin is a respiratory protein in connective tissue and neurons, which is up-regulated by hypoxia. *J. Biol. Chem.* 279, 8063–8069.
- (6) Singh, S., Manda, S. M., Sikder, D., Birrer, M. J., Rothermel, B. A., Garry, D. J., and Mammen, P. P. (2009) Calcineurin activates

cytoglobin transcription in hypoxic myocytes. *J. Biol. Chem.* 284, 10409–10421.

(7) Pesce, A., Bolognesi, M., Bocedi, A., Ascenzi, P., Dewilde, S., Moens, L., Hankeln, T., and Burmester, T. (2002) Neuroglobin and cytoglobin. Fresh blood for the vertebrate globin family. *EMBO Rep.* 3, 1146–1151.

(8) Smagghe, B. J., Trent, J. T., III, and Hargrove, M. S. (2008) NO dioxygenase activity in hemoglobins is ubiquitous in vitro, but limited by reduction in vivo. *PLoS One* 3, e2039.

(9) Halligan, K. E., Jourdain, F. L., and Jourdain, D. (2009) Cytoglobin is expressed in the vasculature and regulates cell respiration and proliferation via nitric oxide dioxygenation. *J. Biol. Chem.* 284, 8539–8547.

(10) Gardner, A. M., Cook, M. R., and Gardner, P. R. (2010) Nitric-oxide dioxygenase function of human cytoglobin with cellular reductants and in rat hepatocytes. *J. Biol. Chem.* 285, 23850–23857.

(11) Fordel, E., Thijs, L., Moens, L., and Dewilde, S. (2007) Neuroglobin and cytoglobin expression in mice. Evidence for a correlation with reactive oxygen species scavenging. *FEBS J.* 274, 1312–1317.

(12) Herold, S., Fago, A., Weber, R. E., Dewilde, S., and Moens, L. (2004) Reactivity studies of the Fe(III) and Fe(II)NO forms of human neuroglobin reveal a potential role against oxidative stress. *J. Biol. Chem.* 279, 22841–22847.

(13) Burmester, T., Gerlach, F., and Hankeln, T. (2007) Regulation and role of neuroglobin and cytoglobin under hypoxia. *Adv. Exp. Med. Biol.* 618, 169–180.

(14) Petersen, M. G., Dewilde, S., and Fago, A. (2008) Reactions of ferrous neuroglobin and cytoglobin with nitrite under anaerobic conditions. *J. Inorg. Biochem.* 102, 1777–1782.

(15) Alzawhra, W. F., Talukder, M. A., Liu, X., Samouilov, A., and Zweier, J. L. (2008) Heme proteins mediate the conversion of nitrite to nitric oxide in the vascular wall. *Am. J. Physiol.* 295, H499–H508.

(16) Liu, X., Srinivasan, P., Collard, E., Grajdeanu, P., Lok, K., Boyle, S. E., Friedman, A., and Zweier, J. L. (2010) Oxygen regulates the effective diffusion distance of nitric oxide in the aortic wall. *Free Radical Biol. Med.* 48, 554–559.

(17) Thomas, D. D., Liu, X., Kantrow, S. P., and Lancaster, J. R., Jr. (2001) The biological lifetime of nitric oxide: Implications for the perivascular dynamics of NO and O<sub>2</sub>. *Proc. Natl. Acad. Sci. U.S.A.* 98, 355–360.

(18) Taylor, C. T., and Moncada, S. (2010) Nitric oxide, cytochrome C oxidase, and the cellular response to hypoxia. *Arterioscler., Thromb., Vasc. Biol.* 30, 643–647.

(19) Lima, B., Forrester, M. T., Hess, D. T., and Stamler, J. S. (2010) S-nitrosylation in cardiovascular signaling. *Circ. Res.* 106, 633–646.

(20) van Faassen, E. E., Bahrami, S., Feelisch, M., Hogg, N., Kelm, M., Kim-Shapiro, D. B., Kozlov, A. V., Li, H., Lundberg, J. O., Mason, R., Nohl, H., Rassaf, T., Samouilov, A., Slama-Schwok, A., Shiva, S., Vanin, A. F., Weitzberg, E., Zweier, J., and Gladwin, M. T. (2009) Nitrite as regulator of hypoxic signaling in mammalian physiology. *Med. Res. Rev.* 29, 683–741.

(21) Brunori, M., Giuffrè, A., Nienhaus, K., Nienhaus, G. U., Scandurra, F. M., and Vallone, B. (2005) Neuroglobin, nitric oxide, and oxygen: Functional pathways and conformational changes. *Proc. Natl. Acad. Sci. U.S.A.* 102, 8483–8488.

(22) Lechaue, C., Chauvierre, C., Dewilde, S., Moens, L., Green, B. N., Marden, M. C., Celier, C., and Kiger, L. (2010) Cytoglobin conformations and disulfide bond formation. *FEBS J.* 277, 2696–2704.

(23) Fago, A., Hundahl, C., Malte, H., and Weber, R. E. (2004) Functional properties of neuroglobin and cytoglobin. Insights into the ancestral physiological roles of globins. *IUBMB Life* 56, 689–696.

(24) Wink, D. A., Darbyshire, J. F., Nims, R. W., Saavedra, J. E., and Ford, P. C. (1993) Reactions of the bioregulatory agent nitric oxide in oxygenated aqueous media: Determination of the kinetics for oxidation and nitrosation by intermediates generated in the NO/O<sub>2</sub> reaction. *Chem. Res. Toxicol.* 6, 23–27.

(25) Goldstein, S., and Czapski, G. (1995) Kinetics of Nitric Oxide Autoxidation in Aqueous Solution in the Absence and Presence of

Various Reductants. The Nature of the Oxidizing Intermediates. *J. Am. Chem. Soc.* 117, 12078–12084.

(26) Liu, X., Liu, Q., Gupta, E., Zorko, N., Brownlee, E., and Zweier, J. L. (2005) Quantitative measurements of NO reaction kinetics with a Clark-type electrode. *Nitric Oxide* 13, 68–77.

(27) Liu, X., El-Sherbiny, G. A., Colard, E., Huang, X., Follmer, D., El-Mahdy, M., and Zweier, J. L. (2010) Application of carbon fiber composite minielectrodes for measurement of kinetic constants of nitric oxide decay in solution. *Nitric Oxide* 23, 311–318.

(28) Gardner, A. M., Martin, L. A., Gardner, P. R., Dou, Y., and Olson, J. S. (2000) Steady-state and transient kinetics of *Escherichia coli* nitric-oxide dioxygenase (flavo-hemoglobin). The B10 tyrosine hydroxyl is essential for dioxygen binding and catalysis. *J. Biol. Chem.* 275, 12581–12589.

(29) Doyle, M. P., Pickering, R. A., and Cook, B. R. (1983) Oxidation of oxymyoglobin by nitric oxide through dissociation from cobalt nitrosyls. *J. Inorg. Biochem.* 19, 329–338.

(30) Eich, R. F., Li, T., Lemon, D. D., Doherty, D. H., Curry, S. R., Aitken, J. F., Mathews, A. J., Johnson, K. A., Smith, R. D., Phillips, G. N., Jr., and Olson, J. S. (1996) Mechanism of NO-induced oxidation of myoglobin and hemoglobin. *Biochemistry* 35, 6976–6983.

(31) Doyle, M. P., and Hoekstra, J. W. (1981) Oxidation of nitrogen oxides by bound dioxygen in hemoproteins. *J. Inorg. Biochem.* 14, 351–358.

(32) Hamdane, D., Kiger, L., Dewilde, S., Green, B. N., Pesce, A., Uzan, J., Burmester, T., Hankeln, T., Bolognesi, M., Moens, L., and Marden, M. C. (2003) The redox state of the cell regulates the ligand binding affinity of human neuroglobin and cytoglobin. *J. Biol. Chem.* 278, 51713–51721.

(33) Uzan, J., Dewilde, S., Burmester, T., Hankeln, T., Moens, L., Hamdane, D., Marden, M. C., and Kiger, L. (2004) Neuroglobin and other hexacoordinated hemoglobins show a weak temperature dependence of oxygen binding. *Biophys. J.* 87, 1196–1204.

(34) Fago, A., Hundahl, C., Dewilde, S., Gilany, K., Moens, L., and Weber, R. E. (2004) Allosteric regulation and temperature dependence of oxygen binding in human neuroglobin and cytoglobin. Molecular mechanisms and physiological significance. *J. Biol. Chem.* 279, 44417–44426.

(35) Moore, E. G., and Gibson, Q. H. (1976) Cooperativity in the dissociation of nitric oxide from hemoglobin. *J. Biol. Chem.* 251, 2788–2794.

(36) Van Doorslaer, S., Dewilde, S., Kiger, L., Nistor, S. V., Goovaerts, E., Marden, M. C., and Moens, L. (2003) Nitric oxide binding properties of neuroglobin. A characterization by EPR and flash photolysis. *J. Biol. Chem.* 278, 4919–4925.

(37) Farres, J., Rechsteiner, M. P., Herold, S., Frey, A. D., and Kallio, P. T. (2005) Ligand binding properties of bacterial hemoglobins and flavohemoglobins. *Biochemistry* 44, 4125–4134.

(38) Gardner, P. R., Martin, L. A., Hall, D., and Gardner, A. M. (2001) Dioxygen-dependent metabolism of nitric oxide in mammalian cells. *Free Radical Biol. Med.* 31, 191–204.

(39) Liu, X. P., Srinivasan, P., Collard, E., Grajdeanu, P., Zweier, J. L., and Friedman, A. (2007) Oxygen regulates the flux of nitric oxide diffusion across the vascular wall. *Circulation* 116, 27–27.

(40) Lawrie, R. A. (1998) *Lawrie's meat science*, 6th ed., Woodhead Publishing, Cambridge, U.K.

(41) Khaw, K. T., and Woodhouse, P. (1995) Interrelation of vitamin C, infection, haemostatic factors, and cardiovascular disease. *BMJ [Br. Med. J.]* 310, 1559–1563.

(42) Frei, B., Stocker, R., England, L., and Ames, B. N. (1990) Ascorbate: The most effective antioxidant in human blood plasma. *Adv. Exp. Med. Biol.* 264, 155–163.

(43) Bobrowicz, E., Naskalski, J. W., and Siedlecki, A. (2001) Preanalytical factors in human plasma ascorbate assay. *Clin. Chim. Acta* 314, 237–239.

(44) Evelson, P., Travacio, M., Repetto, M., Escobar, J., Llesuy, S., and Lissi, E. A. (2001) Evaluation of total reactive antioxidant potential (TRAP) of tissue homogenates and their cytosols. *Arch. Biochem. Biophys.* 388, 261–266.



- (45) May, J. M., Qu, Z. C., and Qiao, H. (2009) Transfer of ascorbic acid across the vascular endothelium: Mechanism and self-regulation. *Am. J. Physiol.* 297, C169–C178.
- (46) Welch, R. W., Bergsten, P., Butler, J. D., and Levine, M. (1993) Ascorbic acid accumulation and transport in human fibroblasts. *Biochem. J.* 294 (Part 2), 505–510.
- (47) Qiao, H., Bell, J., Juliao, S., Li, L., and May, J. M. (2009) Ascorbic acid uptake and regulation of type I collagen synthesis in cultured vascular smooth muscle cells. *J. Vasc. Res.* 46, 15–24.
- (48) Barnes, H. J., Arlotto, M. P., and Waterman, M. R. (1991) Expression and enzymatic activity of recombinant cytochrome P450 17 $\alpha$ -hydroxylase in *Escherichia coli*. *Proc. Natl. Acad. Sci. U.S.A.* 88, 5597–5601.
- (49) McGuire, J. J., Anderson, D. J., McDonald, B. J., Narayanasami, R., and Bennett, B. M. (1998) Inhibition of NADPH-cytochrome P450 reductase and glyceryl trinitrate biotransformation by diphenyleneiodonium sulfate. *Biochem. Pharmacol.* 56, 881–893.
- (50) Tsai, A. C., and Kelley, J. J. (1978) Effect of cholesterol feeding on hepatic fatty acid synthesis and serum and tissue enzyme activities in rabbits. *J. Nutr.* 108, 226–231.
- (51) Lee, M. J., and Dinsdale, D. (1995) The subcellular distribution of NADPH-cytochrome P450 reductase and isoenzymes of cytochrome P450 in the lungs of rats and mice. *Biochem. Pharmacol.* 49, 1387–1394.
- (52) Loeper, J., Louerat-Oriou, B., Duport, C., and Pompon, D. (1998) Yeast expressed cytochrome P450 2D6 (CYP2D6) exposed on the external face of plasma membrane is functionally competent. *Mol. Pharmacol.* 54, 8–13.
- (53) Buerk, D. G., Lamkin-Kennard, K., and Jaron, D. (2003) Modeling the influence of superoxide dismutase on superoxide and nitric oxide interactions, including reversible inhibition of oxygen consumption. *Free Radical Biol. Med.* 34, 1488–1503.
- (54) Tsoukias, N. M., Kavdia, M., and Popel, A. S. (2004) A theoretical model of nitric oxide transport in arterioles: Frequency- vs. amplitude-dependent control of cGMP formation. *Am. J. Physiol.* 286, H1043–H1056.
- (55) Vaughn, M. W., Kuo, L., and Liao, J. C. (1998) Effective diffusion distance of nitric oxide in the microcirculation. *Am. J. Physiol.* 274, H1705–H1714.